Proceedings of the World Congress on Engineering 2010 Vol II
WCE 2010, June 30 - July 2, 2010, London, U.K.

Study on Energy Storage Hybrid Wind Power Generation Systems

Hao Sun, Jihong Wang*, Shen Guo and Xing Luo

***Abstract*— Wind energy has been considered as a clean and inexhaustible energy source for electrical power generation and its penetration level has increased dramatically worldwide in recent years. However, its nature of intermittence is still a universally faced challenge. As a possible solution, energy storage technology integrating with renewable power generation process is considered as one of options in recent years. The paper aims to study and compare two feasible energy storage means - compressed air (CAES) and electrochemical energy storage (ECES) for wind power generation applications. A novel CAES structure in hybrid connection with a smaller power scale wind turbine is proposed. The mathematical model for the combined wind turbine system is developed and the system performance simulation study is given. Also, a pneumatic power compensation control strategy is reported to achieve acceptable power output quality and smooth mechanical connection transition.**

***Index Terms*— wind turbines, compressed air energy storage, electrochemical energy storage, system modeling.**

I. INTRODUCTION

Nowadays, the world is facing the challenge to meet the continuously increasing energy demand and to reduce the harmful impact to our environment. The difficulty encountered in matching energy supply with demand becomes more complex while renewable energy power generation is involved due to its nature of fluctuation intermittency. And in particular, wind energy appears as preferable solution to take an considerable portion of the generation market, especially in the UK. Multifarious wind turbine concepts have been developed; single-machine capacity can vary from 1kW to 7MW. However, the key challenge faced by all kinds of wind power generations is intermittency. Figure 1 shows typical hourly variations case in wind power production for Western Denmark. It can be seen that the generated power from wind exceeded power consumption on several occasions. Nevertheless, there were vast majority of periods with low and no wind in January. Besides this, energy regulatory policies all around the world have been characterized by the introduction of competition in the power industry and market, both at the wholesale and at the retail levels. The variable market brought another complex factor to the power network. Undesirable impacts onto power transmission and distribution networks have been studied at length ([1] [2]). It is highly desired to alleviate such impacts through alternative technologies.

Hao Sun, Jihong Wang*, Shen Guo and Xing Luo are currently with the School of Electronic, Electrical and Computer Engineering, University of Birmingham, Edgbaston, Birmingham B15 2TT, UK.
* The author for correspondence, email: j.h.wang@bham.ac.uk

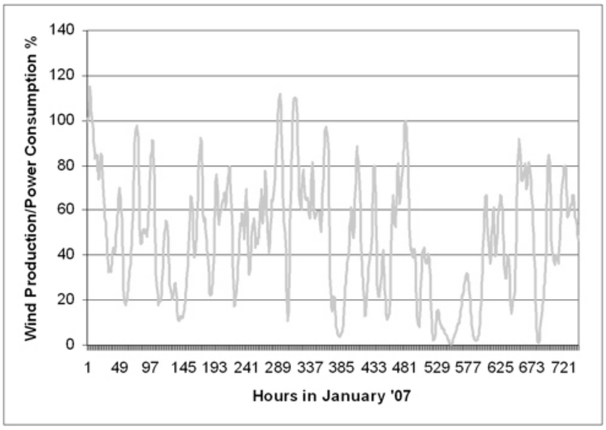

Figure1: Wind Power as a Percentage of Domestic Power Consumption in January 2007, Hourly Basis, Source: Risø DTU [3]

One proposed solution is to introduce an element of storage or an alternative supply for use when the ambient flux is insufficient for a guaranteed supply to the demand. The primary cause is that energy storage can make wind power available when it is most demanded. Apart from the pumped water, battery, hydrogen and capacitors for energy storage, ccompressed air energy storage (CAES) is also a well known controllable and affordable technology ([4] [5] [6]). In a CAES system, the excess power is used to compress air which can be stored in a vessel or a cavern. The energy stored in compressed air will be used to generate electricity when required. Compared with other types of energy storage schemes, CAES is sustainable and will not produce any chemical waste. However, energy conversion always results in energy loss because it is almost impossible to achieve 100% efficiency, technically. In this paper, a comparative analysis between CAES and electrochemical storage has been conducted. A hybrid energy storage wind turbine system is proposed in the paper, which connects a typical wind turbine and vane-type air motor. The mathematical model for the whole system is derived and simulation study is conducted. The study of such a CAES system has shown the promising merit of the proposed hybrid connection of wind turbines and CAES.

II. ELECTROCHEMICAL AND COMPRESSED AIR ENERGY STORAGE

In this paper, the feasibility of energy storage for 2kW household small scale wind turbine is analysed. Electrochemical energy storage (ECES) is the most popular type of energy storage in the world from small to large scales. For instance, the lead-acid batteries are the oldest rechargeable battery with widest range of applications and

ISBN: 978-988-18210-7-2
ISSN: 2078-0958 (Print); ISSN: 2078-0966 (Online)

the lead-acid battery is a mature and cost-effective choice among all the battery types. The main advantages of ECES are none emission for air pollutions, simple in operation and higher energy efficiency. The efficiency of lead-acid batteries is generally around 80%. CAES is clean and no emission pollutions and also no chemical disposal pollution to environment ([7]). While, the compressed air energy storage system has much lower energy efficiency; much energy is lost during the process of energy conversion ([8] [9] [10]).

A drawback ECES faced is relatively short lifetime that mainly expressed on the limited charge/discharge cycle life. For example, lead-acid battery's cycle life is roughly in the range of 500-1500. This issue can be more serious when it is applied to wind power generation due to the high variation in wind speed and low predictability to the wind power variation patterns, that is, the battery will be frequently charged and discharged. For CAES, the pneumatic actuators, including compressor, air motor, tank, pipes and valves, are relatively robust; the major components have up to 50-year lifetime. Therefore, the whole system lift time would be only determined by the majority of the mechanical components in the system.

The capacity of an electrochemical battery is directly related to the active material in the battery. That means the more energy the battery can offer, the more active material will be contained in the battery, and therefore the size, weight as well as the price is almost linear versus the battery capacity. For the compressed air system, the capacity correlates to the volume of tank. Even though the pneumatic system also requires large space to sustain a long term operation, but it has been proven more cost-effective in consideration of the practically free raw material (see Table 1 [11]).

Table1. Typical marginal energy storage costs

Types	Overall cost
Electro-chemical Storage:	>$400/KWh
Pumped Storage:	$80/KWh
Compressed Air :	$1/KWh

The electromotive force of a lead-acid cell provides only about two Volts voltage due to its electrochemical characteristics, and enormous amount of cells therefore should be connected in series to obtain a higher terminal voltage. With this series connection, if one cell within the battery system goes wrong, the whole battery may fail to store or offer energy in the manner desired. Discouragingly, it is very hard currently to diagnose which cell in the system fails and it is expensive and not cost-effective to replace the whole pack of batteries. Besides, most lead-acid batteries designed for the deep discharge are not sealed, and the regular maintenance is therefore required due to the gas emission caused by the water electrolysis while overcharged. Comparing with these characteristics of batteries, CAES only needs regular leakage test and oil maintenance. In brief, a comparison between CAES and ECES can be summarized in Table 2.

III. THE HYBRID WIND TURBINE SYSTEM WITH CAES

There are two possible system structures for a hybrid wind turbine system with compressed air energy storage; one has been demonstrated as an economically solution for utility-scale energy storage on the hours' timescale. The energy storage system application diagram is illustrated in Figure 2.

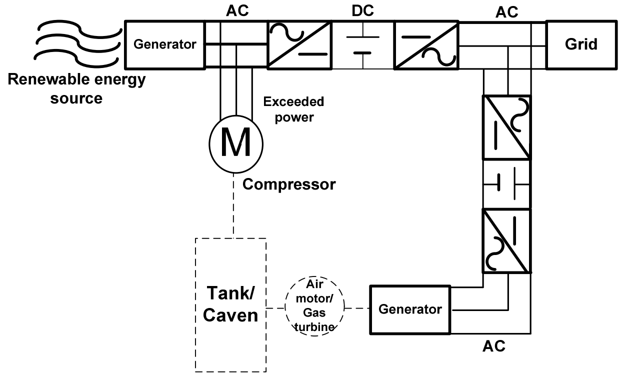

Figure 2: Utility-scale CAES application's diagram

Such systems are successfully implemented in Hantorf in Germany, McIntosh in Alabama, Norton in Ohio, a municipality in Iowa, in Japan and under construction in Israel [12]. The CAES produces power by storing energy in the form of compressed air in an underground cavern. Air is compressed during off-peak periods, and is used on compensating the variation of the demand during the peak periods to generate power with a turbo-generator/gas turbine system. However, this system seems to be disadvantageous as it needs a large space to store compressed air, such as large underground carven for large scale power facilities. So this may limit its applications in terms of site installation. Besides all the above mentioned issues, large-capacity converter and inverter systems are neither cost effective nor power effective.

Table2. Comparison between compressed air (CAES) and electrochemical energy storage (ECES)

	CAES	ECES
Service life	Long	Short
Efficiency	Not high	Very high
Size	Large depend on tank size	Large depend on cell number
Overall cost	Very cheap	Very expensive
maintenance	Need regular maintenance	Hard to overhaul, Need regular maintenance

For smaller capacity of wind turbines, this paper presents a novel hybrid technology to engage energy storage to wind power generation. As shown in Figure 3, the electrical and pneumatic parts are connected through a mechanical transmission mechanism. This electromechanical integration offers simplicity of design, therefore, to ensure a higher efficiency and price quality. Also, the direct compensation of torque variation of the wind turbine will alleviate the stress imposed onto the wind turbine mechanical parts.

ISBN: 978-988-18210-7-2
ISSN: 2078-0958 (Print); ISSN: 2078-0966 (Online)

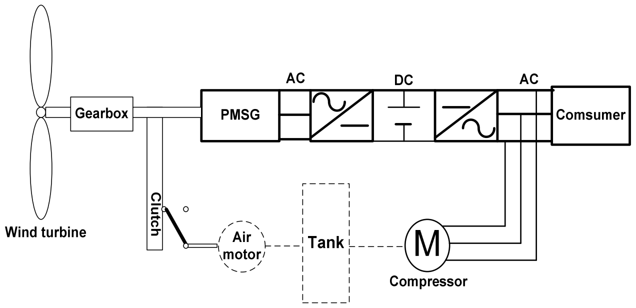

Figure 3: Small scale hybrid wind turbine with CAES

IV. MODELLING STUDY OF THE HYBRID SYSTEM

For the system proposed in III, the complete mathematical model has been derived, which is used to test the practicability of the whole hybrid system concept. At this stage, the system is designed to include a typical wind turbine with permanent magnetic synchronous generator (PMSG), vane type air motor and mechanical power transmission system. The pneumatic system can work as power compensation during the low wind power period. The whole system mathematical model is developed and described below.

i. Mathematical model of the wind turbine:

For a horizontal axis wind turbine, the mechanical power output P that a turbine can produce in steady state is given by:

$$P = \frac{1}{2}\rho \pi r_T{}^2 v_w^3 C_p \tag{1}$$

where ρ is the air density, v_w is wind speed, r_T is the blade radius; C_p reveals the capability of turbine for obtaining energy from wind. This coefficient depends on the tip speed ratio $\lambda = \omega_T r_T / v_w$ and the blade angle, ω_T denotes the turbine speed. This aerodynamic model is based on C_p curves for the constant pitch rotor blades. The model of rotor blades is based on Proven 2.5 type (Proven Energy Ltd [13]), which has the rated power of 2.2kW at 10m/s.

To describe the impact of the dynamic behaviors of the wind turbine, a simple drive train model is considered.

$$\frac{d}{dt}\omega_T = \frac{1}{J_T}(T_T - T_L - B\omega_T) \tag{2}$$

where J_T is the inertia of turbine blades, T_T and T_L mean the torque of turbine and low speed shaft respectively, B is the damping coefficient of the driven train system.

ii. Modelling the permanent magnetic synchronous generator (PMSG)

The model of a PMSG with pure resistance load (for simplicity of analysis) is formed of the following equations.

For the mechanical part:

$$\frac{d}{dt}\omega_G = \frac{1}{J_G}(T_G - T_e - F\omega_G) \tag{3}$$

$$\frac{d\theta_G}{dt} = \omega_G \tag{4}$$

For the electrical part:

$$\frac{d}{dt}i_d = \frac{1}{L_d}v_d - \frac{R_s}{L_d}i_d + \frac{L_q}{L_d}p\omega_G i_q \tag{5}$$

$$\frac{d}{dt}i_q = \frac{1}{L_q}v_q - \frac{R_s}{L_q}i_q - \frac{L_d}{L_q}p\omega_G i_d - \frac{\varepsilon p\omega_G}{L_q} \tag{6}$$

$$T_e = 1.5p[\varepsilon i_q + (L_d - L_q)i_d i_q] \tag{7}$$

$$V_q = \frac{1}{3}[\sin(p\theta_G)\cdot(2V_{ab} + V_{bc}) + \sqrt{3}V_{bc}\cos(p\theta_G)] \tag{8}$$

$$V_d = \frac{1}{3}[\cos(p\theta_G)\cdot(-2V_{ab} - V_{bc}) - \sqrt{3}V_{bc}\sin(p\theta_G)] \tag{9}$$

where, θ_G and ω_G are generator rotating angle and speed, F means the combined viscous friction of rotor and load, i is current, v means voltage, L is inductance, R_s is resistance of stator windings, p is the number of pole pairs of the generator, ε is the amplitude of the flux induced by the permanent magnets of the rotor in the stator phases. While, the subscripts a, b, c, d, q represent the axes of a, b, c, d, q for different electrical phases. The three-phase coordinates and dq rotating coordinates can be transformed each other through Park's transformation [14].

iii. Model of the vane-type air motor:

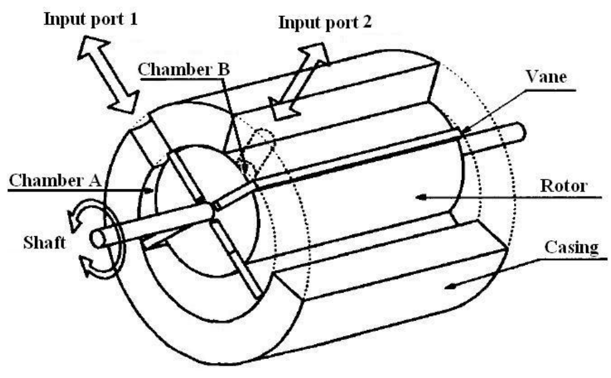

Figure 4: Structure of a vane type air motor with four vanes

Figure 4 shows the sketch of a vane-type air motor with four vanes. There is a rotational drive shaft with four slots, each of which is fitted with a freely sliding rectangular vane. When the drive shaft starts to rotate, the vanes tend to slide outward due to centrifugal force and are limited by the shape of the rotor housing. Depending on the flow direction, this motor will rotate in either clockwise or counter clockwise directions. In this part, input port 1 is supposed to be the inlet port, and then input port 1 will be outlet port. Compressed air is admitted through the input port1 from servo valves and fills the cavity between the vanes, housing and rotor. The chamber A which is open to the input port 1 fills up under high pressure. Once the port is closed by the moving vane, the air expands to a lower pressure in a higher volume between the vane and the preceding vane, at which point the air is released via the input port 2. The difference in air pressure acting on the vane results in a torque acting on the rotor shaft ([15] [16]).

ISBN: 978-988-18210-7-2
ISSN: 2078-0958 (Print); ISSN: 2078-0966 (Online)

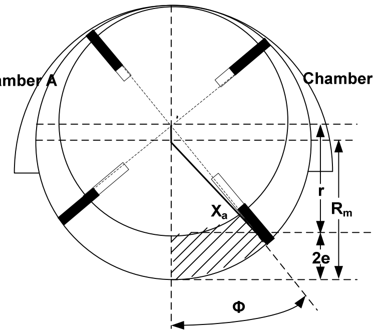

Figure 5: Schematic diagram of the structure of a vane-type air motor

A simplified vane motor structure is shown in Figure 5. The vane working radius measured from the rotor centre, x_a can be derived by:

$$x_a = e\cos\phi + \sqrt{R_m{}^2 - e^2\sin^2\phi} \tag{10}$$

The volumes of chamber *A* and chamber *B* are derived as follows, and presented by the subscription *a* and *b* in this part equations.

$$V_a == \frac{1}{2}L(R_m{}^2 - r^2)(\pi + \phi) + \frac{1}{4}L_m e^2 \sin 2\varphi + L_m e R_m \sin\varphi \tag{11}$$

$$V_b = \frac{1}{2}L_m(R_m{}^2 - r^2)(\pi - \phi) - \frac{1}{4}L_m e^2 \sin 2\varphi - L_m e R_m \sin\varphi\pi \tag{12}$$

where, R_m is radius of motor body; *e* is eccentricity; L_m is vane active length in the axial direction, ϕ is motor rotating angle, *r* means rotor radius .

The pressure of chamber A and B can be derived [10]:

$$\dot{P}_a = -\frac{k\dot{V}_a}{V_a}P_a + \frac{k}{V_a}RT_sC_dC_0A_aX_a f(P_a, P_s, P_e) \tag{13}$$

$$\dot{P}_b = -\frac{k\dot{V}_b}{V_b}P_b + \frac{k}{V_b}RT_sC_dC_0A_bX_b f(P_b, P_s, P_e) \tag{14}$$

where, T_s is supply temperature, *R*, C_d, C_0 are air constant, *A* is effective port width of control valve, *X* is valve spool displacement, *f* is a function of the ratio between the downstream and upstream pressures at the orifice.

The drive torque is determined by the difference of the torque acting on the vane between the drive and exhaust chambers, and is given by [13]:

$$M = (P_a - P_b)(e^2\cos 2\varphi + 2eR_m\cos\varphi + R_m{}^2 - r^2)L/2 \tag{15}$$

iv. Model of mechanical power transmission:

The power transmission system, which is similar to a vehicle air conditioning system, includes clutch and belt speed transmission to ensure coaxial running, as shown in Figure 6([17]).

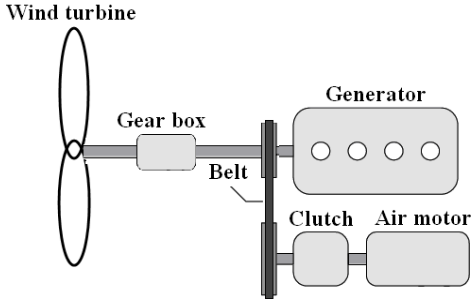

Figure 6: The structure of the power transmission system in hybrid wind turbine

When there is lack of natural wind power, the pneumatic control valve will open; then the scroll air motor is started, working as power compensation to the wind turbine. The clutch can be engaged only when the turbine and air motor operates at the same speed for the purpose of avoiding mechanical damage. Even so, the system design still faces another challenge during the engagement, that is, the speed of air motor could not reach a speed as high as the turbine generator does, in most instances. Therefore, the two plates of belt transmission are designed in different diameters to play the function as a gearbox. The main issue of modelling the power transmission is that two different configurations are presented:

Case I. Clutch disengaged: After the air motor has started during the period before the two sides of electromagnetic clutch get the same speed, the clutch can be considered completely separated. While the scroll air motor is operating at the idle statue with the inertia load of clutch friction plate. Considering friction and different payloads applying Newton's second law of angular motion, we have

$$M - M_f\dot{\phi} = (J_a + J_f)\ddot{\phi} \tag{16}$$

where J_a is the air motor inertia, J_f is friction plate inertia, M is the drive torque, M_f is the friction coefficient, $\dot{\phi}$ is the angular velocity, $\ddot{\phi}$ represents the angular acceleration.

Both the active plate and passive plate of the belt transmission can be considered as the generator inertia load, so the total equivalent inertia is

$$J_{total} = J_{pass} + i^2 J_{act} \tag{17}$$

where J_{pass} and J_{act} is the inertia of passive and active plate respectively, and i is the speed ratio of the belt.

Case II. Clutch engaged: Once the angular velocity of air motor $\dot{\phi}$ meets that of active plate ω_G / i , the clutch will be engaged with the two sides. After the engagement, the active plate and friction plate can be assumed together to be one mass. The dynamic equations are as follows:

$$\begin{cases} M - M_f\dot{\phi} - T_{act} = (J_a + J_f + J_{act})\ddot{\phi} \\ T_{pass} = \dfrac{T_{act}\eta}{i} \\ \dfrac{d\omega_G}{dt} = \dfrac{1}{J_G + J_{pass}}(T_H + T_{pass} - T_e - F\omega_G) \\ \dot{\phi} = \dfrac{\omega_G}{i} \end{cases}$$

where, T_H is the input torque of wind turbine high speed shaft, η is the transfer efficiency of the belt.

Choose system state variables to be x_1: pressure in the chamber A, x_2: pressure in the chamber B, x_3: rotated angle, x_4: angular speed, x_5: current in d axis, x_6: current in q axis. And input variables u_1: wind speed, u_2: input valve displacement. Combining the wind turbine, driven train and

ISBN: 978-988-18210-7-2
ISSN: 2078-0958 (Print); ISSN: 2078-0966 (Online)

generator models together, the state functions of the whole hybrid wind turbine system can then be described by:

$$\dot{x}_1 = -\frac{k\dot{V}_a}{V_a} x_1 + \frac{k}{V_a} RT_s C_d C_0 A_a u_2 f(P_a, P_s, P_e)$$

$$\dot{x}_2 = -\frac{k\dot{V}_b}{V_b} x_2 + \frac{k}{V_b} RT_s C_d C_0 A_b X_b f(P_b, P_s, P_e)$$

$$\dot{x}_3 = \frac{x_4}{i}$$

$$\dot{x}_4 = \frac{1}{J_G + J_{pass} + J_T \frac{\eta'}{i'^2} + (J_a + J_f + J_{act}) \frac{\eta}{i^2}} \left\{ \eta \frac{\rho \pi r^2 u_1^3 C_p'}{2x_5} - \eta \frac{B' x_4}{i'^2} + \eta \frac{M}{i} - \eta \frac{M_f x_4}{i^2} - M_c S(\frac{x_4}{i}) - \frac{3}{2} p(\varepsilon x_6 + L_d x_6 x_5 - L_q x_6 x_5) - F x_4 \right\}$$

$$\dot{x}_5 = \frac{v_d}{L_d} - \frac{R_s}{L_d} x_5 + \frac{L_q}{L_d} p x_4 x_6$$

$$\dot{x}_6 = \frac{v_q}{L_q} - \frac{R_s}{L_q} x_6 - \frac{L_d}{L_q} p x_4 x_5 - \frac{\varepsilon p x_5}{L_q}$$

where, η', i' is the efficiency and speed ratio of wind turbine gearbox. With such a complicated structure of the system model, sometimes, it is difficult to obtain accurate values of system parameters. Intelligent optimization and identification methods have been proved to be an effective method to tackle this challenging problem ([18] [19]). The test system for the proposed hybrid system structure is under development in the authors' laboratory and the data obtained from the rig can be used to improve the model accuracy.

V. Simulation Study

The proposed hybrid wind turbine system and the model derived above is implemented in MATLAB/ SIMULINK environment to observe the dynamic behavior of the whole system as shown in Figure 7. The simulation results are described below.

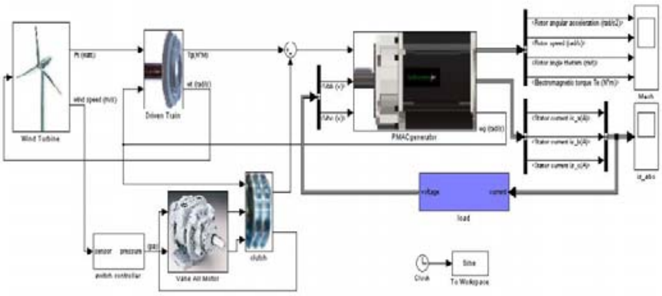

Figure 7: The block diagram of the simulation system

The simulation considers the scenario when the input wind speed steps down within a 40 seconds' time series observation window, that is, drops from 9 to 8 m/s at the time of 20 seconds and the whole simulation time period is 40 seconds (see Figure 8).

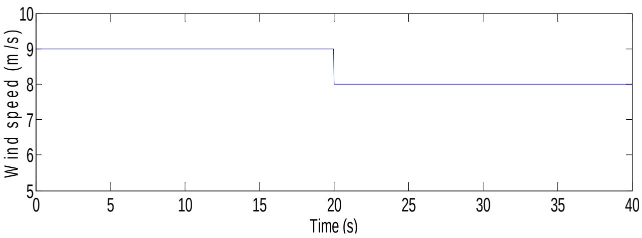

Figure 8: Input wind speed

For comparison, the results from hybrid system and those from stand-alone system without pneumatic actuators are shown in Figure 9. It can be seen that, the hybrid system can still obtain a high turbine speed due to the contribution of air motor output; also it can maintain a steady value even the natural wind speed decreases. Regrettably, however, the power coefficient of turbine falls because of the increased tip speed ratio $\lambda = \omega_T r_T / v_w$. That should be considered as adverse effect of the hybrid system.

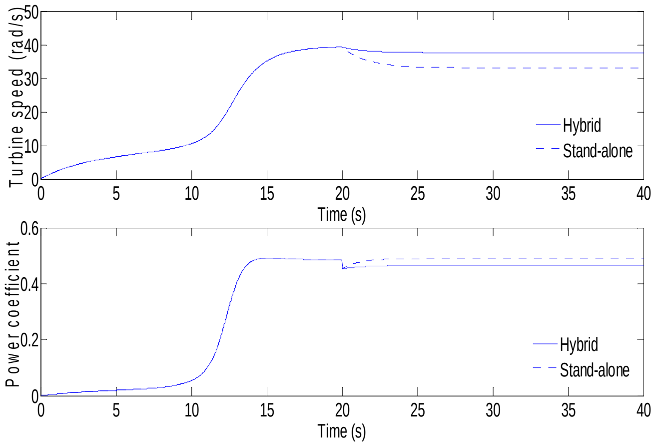

Figure 9: Simulation results of wind turbine

Figure10 provides a significant contrast between hybrid and independent status through generator operation. It can be seen that the power compensation can almost overcome the energy shortfall at the lower wind speed.

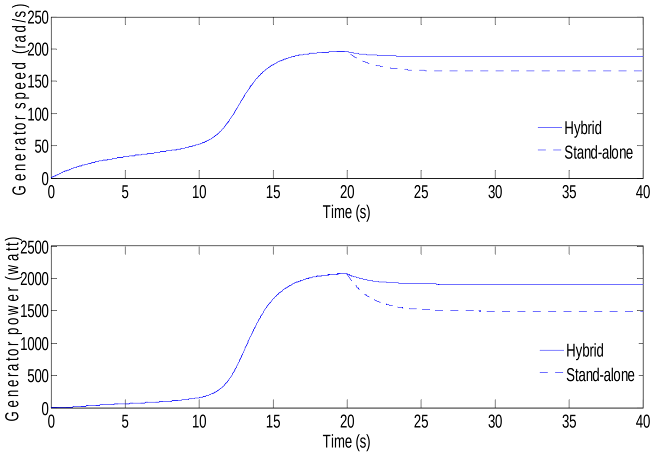

Figure10: Simulation results of the responses of the PMSG

Figure 11 reveals the simulation results of vane type air motor. The air motor started at the time of 20 second, and joined the wind turbine system rapidly owing to its fast response characteristic. It is worth noting that this type of air motor should generally running with wellmarked periodic fluctuation, which is originated from the cyclically changed difference between P_a and P_b (the pressures in chamber A and chamber B). However, in hybrid system, the air motor operates rather smoothly which may be resulted from the large inertia of the whole system.

ISBN: 978-988-18210-7-2
ISSN: 2078-0958 (Print); ISSN: 2078-0966 (Online)

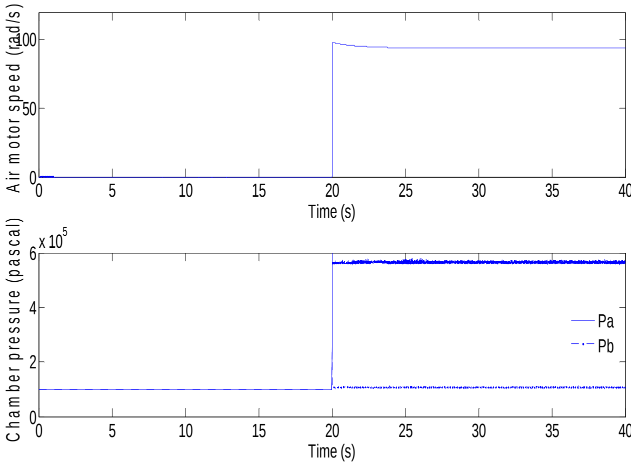

Figure11: Simulation results of vane type air motor

VI. Conclusion

The new concept of CAES applied to small power scale wind turbine system is introduced in the paper. The complete process mathematical model is derived and implemented in MATLAB/SIMULINK environment. The simulation results are very encouraging as the extra power from the air motor output compensates the power shortfall from wind energy. This strategy enables the wind turbine operates at a relatively uniformly distributed speed profile, which in turn will improve the operation condition of the overall system. The simple structure of the system and the advantage of CAES would provide the opportunities for such a system to be placed in the future renewable energy electricity market. The research in hybrid wind turbine is still on-going and further improvement is expected. Advanced tracking control strategy is a promising methodology in consideration of the research team ([7] [20]).

ACKNOWLEDGEMENT:

The authors would like to thank the support from Advantage West Midlands and the European Regional Development Agency for the support of Birmingham Science City Energy Efficiency & Demand Reduction project, China 863 Project (2009AA05Z212) and the scholarships for Hao Sun, Xing Luo from the School of Electronic, Electrical and Computer Engineering, the University of Birmingham, UK.

References

[1]. V. Akhmatov, “Variable-speed wind turbines with doubly-fed induction generators. Part II: Power system stability”, *Wind Eng*, vol. 26, No.3, pp. 71–88, 2002.

[2]. A. D. Hansena and G. Michalke, “Fault ride-through capability of DFIG wind turbines”, *Renewable Energy*, vol. 32, pp. 1594-1610, 2007.

[3]. Wind Energy – The Facts, [Online]. Available at: http://www.wind-energy-the-facts.org/en/part-3-economics-of-wind-power/chapter-5-wind-power-at-the-spot-market/the-impact-of-wind-power-on-the-power-market-dk-case.html, on 04 March, 2010.

[4]. A. Cavallo , “Controllable and affordable utility-scale electricity from intermittent wind resources and compressed air energy storage (CAES)”, *Energy*, vol. 32, pp. 120-127, 2007.

[5]. S. Lemofouet and A. Rufer , “A hybrid energy storage system based on compressed air and supercapacitors with maximum efficiency point tracking (MEPT)”, *IEEE Transactions on Industrial Electronics*, vol. 53, No.4, pp. 1105-1115, 2006.

[6]. S. Van der Linden , “BulkEnergy storage potential in the USA, current developments and future prospects”, *Energy*, vol. 31, pp. 3446-3457, 2006.

[7]. J. Wang, J. Pu. and P. Moore , “Accurate position control of servo pneumatic actuator systems: an application to food packaging”, *Control Engineering Practice*, Vol.7, No.6, pp699-706, 1999.

[8]. L. Yang, J. Wang, N. Lu, et al, “Energy efficiency analysis of a scroll-type air motor based on a simplified mathematical model”, *World Congress on Engineering 2007*, London, July 02-04, 2007.

[9]. J. Wang, L. Yang, X. Luo, S. Mangan, J.W. Derby, “Mathematical modelling study of scroll air motors and energy efficiency analysis - Part I”, *IEEE-ASME Transactions on Mechatronics*, Digital Object Identifier 10.1109/TMECH.2009.2036608, 2010.

[10]. J. Wang, X. Luo, L. Yang, L. Shpanin, N. Jia, S. Mangan, J.W. Derby, “Mathematical modelling study of scroll air motors and energy efficiency analysis - Part II”, *IEEE-ASME Transactions on Mechatronics*, Digital Object Identifier 10.1109/TMECH.2009. 2036607, 2010.

[11]. A. Price, “The Current Status of Electrical Energy Storage Systems”, *ESA London Meeting*, London, UK, Jan 2009.

[12]. Ben et al, “Transportable compressed air energy storage (TCASE) system driven by a 2500 kW wind turbine”, *Proceeding of international conference on efficiency, cost, optimization, simulation and environment impact of energy system*, 2006.

[13]. Wind Turbines-Proven Energy wind turbine energy, [Online]. Available at: http://www.solarenergyalliance.com/pdf/Proven_Wind_turbine_Brochure.pdf, on 04 March, 2010.

[14]. P. Pillay and R. Krishnan, “Modeling, simulation and analysis of permanent magnet motor drives, part 1: The permanent-magnet synchronous motor drive,” *IEEE Trans. Ind. Applicat.*, vol. 25, pp. 265–273, Mar. /Apr. 1989.

[15]. X. Luo, J. Wang, L. Shpanin, N. Jia, G. Liu, A. Zinober, “Development of a mathematical model for vane-type air motors with arbitrary N vanes”, *Inter. Conf. of Applied and Engineering Mathematics, WCE*, vol. I, London, July 2008.

[16]. J. Wang, J. Pu, P.R. Moore, Z. Zhang, “Modelling study and servo-control of air motor systems”, *Int. J. Control*, vol. 71, No.3, pp459-476, 1998.

[17]. Y. P. B. Yeung, K. W. E. Cheng, W. W. Chan, C. Y. Lam, W. F. Choi and T. W. Ng, Automobile hybrid air conditioning technology, *The Proceedings of the 3rd International Conference on Power Electronics Systems and Applications*, pp116-116, 2009.

[18]. J. L. Wei, J. Wang, Q. H. Wu, G. Oluwanda, and M. Boardman, “Development of a multi-segment coal mill model using an evolutionary computation technique”, *IEEE Transactions on Energy Conversion*, Vol. 22. pp718-727, 2007.

[19]. Y. G. Zhang, Q.H. Wu, J. Wang, J. Oluwanda, D. Matts, and X.X. Zhou, “Coal mill modelling by machine learning based on on-site measurement”, *IEEE Transactions* on Energy Conversion, Vol.17. No.4, pp549-555, 2002.

[20]. J. Wang, U. Kotta, J. Ke, “Tracking control of nonlinear pneumatic actuator systems using static state feedback linearization of the input-output map” *Proceedings of the Estonian Academy of Sciences-Physics Mathematics*, Vol. 56, pp. 47-66, 2007.